INORGANIC CHEMISTRY

# Characterization of hydrogen-substituted silylium ions in the condensed phase

**Qian Wu, Elisabeth Irran, Robert Müller, Martin Kaupp, Hendrik F. T. Klare*, Martin Oestreich***

**Hydrogen-substituted silylium ions are long-sought reactive species. We report a protolysis strategy that chemoselectively cleaves either an Si–C($sp^2$) or an Si–H bond using a carborane acid to access the full series of $[CHB_{11}H_5Br_6]^-$-stabilized $R_2SiH^+$, $RSiH_2^+$, and $SiH_3^+$ cations, where bulky *tert*-butyl groups at the silicon atom (R = *t*Bu) were crucial to avoid substituent redistribution. The crystallographically characterized molecular structures of $[CHB_{11}H_5Br_6]^-$-stabilized $tBu_2HSi^+$ and $tBuH_2Si^+$ feature pyramidalization at the silicon atom, in accordance with that of $tBu_3Si^+[CHB_{11}H_5Br_6]^-$. Conversely, the silicon atom in the $H_3Si^+$ cation adopts a trigonal-planar structure and is stabilized by two counteranions. This solid-state structure resembles that of the corresponding Brønsted acid.**

Reactive intermediates play a key role in the understanding of chemical reactions (*1*). Accordingly, knowledge of the nature and reactivity of silylium ions ($R_3Si^+$) (*2*, *3*), the heavier analogs of classical carbenium ions ($R_3C^+$) (*4*), is of fundamental interest. Relative to their carbon homologs, however, the chemistry of silylium ions is much less developed (*2*, *3*). For instance, it took almost one century after the discovery of the first stable carbenium ion, the triphenylmethylium (trityl) cation ($Ph_3C^+$), until evidence of a corresponding silicon congener, the trimesitylsilylium ion ($Mes_3Si^+$; mesityl = 2,4,6-trimethylphenyl), was provided in the condensed phase by Reed, Lambert, and co-workers (*5*, *6*). In contrast, secondary and primary silylium ions with hydrogen substituents at the silicon atom remain unknown (*7*, *8*), presumably because of the lack of a general method to access these reactive species (*9*, *10*). The standard strategy to generate silylium ions is the Bartlett-Condon-Schneider protocol for hydride transfer from a hydrosilane to the trityl cation paired with a weakly coordinating anion ($[WCA]^-$) (*11*, *12*), also known as the Corey reaction (*13*). However, this protocol is mainly limited to trialkyl-substituted hydrosilanes, eventually providing donor-stabilized tetracoordinate silylium ions (Fig. 1A, i, left) (*14*–*19*). Although steric shielding of the empty 3p orbital at the silicon atom using bulky 2,6-disubstituted aryl substituents (i.e., Mes or Dur; duryl = 2,3,5,6-tetramethylphenyl) allows for the formation of strictly tricoordinate ("free") silylium ions (*6*), the high steric demand requires a more elaborate synthetic route, involving remote attack of a strong electrophile ($El^+$) on an allyltriarylsilane, the so-called allyl leaving group approach (Fig. 1A, ii, left) (*20*). A more convenient route to triarylsilylium ions was introduced by the group of Müller, making use of a substituent redistribution reaction in the hydride abstraction of heteroleptic methyl(diaryl)silanes (Fig. 1A, ii, right) (*21*, *22*). This process can also be tuned to deliver donor-stabilized trialkylsilylium ions, as recently reported by our laboratory (Fig. 1A, i, right) (*23*). However, all these approaches invariably lead to triorganosubstituted tertiary silylium ions.

Attempts to generate hydrogen-substituted silylium ions by standard hydride abstraction have failed so far (Fig. 1C) (*9*, *10*), although Jutzi and Bunte accessed a secondary silylium ion by protonation of decamethylsilicocene (**1** → **2**; Fig. 1B) (*7*). However, the extreme sensitivity of the silylium ion **2** impeded its crystallographic characterization, and quantum chemical calculations revealed a nonclassical bonding situation, where the positive charge is intramolecularly stabilized by the π-bonded pentamethylcyclopentadienyl ligands (*8*). Aside from this isolated and unique contribution, secondary and primary silylium ions have been exclusively the subject of theoretical and gas-phase studies (*24*–*26*).

Recently, our group disclosed a protocol for the facile generation of donor-stabilized trialkyl-substituted as well as previously unavailable silyl-substituted silylium ions based on the heterolytic cleavage of activated and even inert Si–C($sp^n$) bonds ($n$ = 1 to 3) by protonation with Reed's carborane acid $[C_6H_6{\cdot}H]^+[CHB_{11}H_5Br_6]^-$ (Fig. 1A, iii) (*27*). Encouraged by this work, we envisioned the synthesis of hydrogen-substituted silylium ions by protolysis of a suitable precursor silane (*28*, *29*). Here, we report the successful implementation of this strategy for the preparation and structural characterization of counteranion-stabilized secondary and primary silylium ions, as well as the simplest silylium ion $H_3Si^+$, the heavier analog of the methylium cation $H_3C^+$ (Fig. 1D).

Previous efforts by Müller and co-workers to generate a secondary silylium ion by classical hydride transfer from dihydrosilanes were unsuccessful, leading either to triarylsilylium ions by the reaction with the aromatic solvent, as in the case of diaryldihydrosilane **3** (**3** → **4**; Fig. 1C) (*9*), or to intramolecular rearrangements, as in the case of cyclic disilyl-substituted dihydrosilane **5** (**5** → **6**; Fig. 1C) (*10*). These studies indicate that the synthesis of hydrogen-substituted silylium ions is hampered by their exceptionally high electrophilicity and tendency to undergo substituent exchange reactions (*21*–*23*). Although the use of sterically hindered aryl substituents and stabilizing silyl substituents turned out to be ineffective, we probed the hydride abstraction from a dialkyl-substituted dihydrosilane and chose di-*tert*-butyldihydrosilane (**7**) as a test substrate, as we knew from our previous study that the bulky *tert*-butyl group prevents any substituent redistribution (*23*). To investigate a possible influence of the counteranion, we used Reed's carborane-based trityl salt $[Ph_3C]^+[CHB_{11}H_5Br_6]^-$ as a hydride abstracting agent. Indeed, the formation of the secondary counteranion-stabilized silylium ion $tBu_2HSi^+[CHB_{11}H_5Br_6]^-$ (**8**) was observed in this case (**7** → **8**; Fig. 1C). However, the reaction was extremely slow, not reaching full conversion even after 2 weeks. Overall, these attempts demonstrate the challenges associated with the synthesis of hydrogen-substituted silylium ions.

The efficiency of our recently introduced method to generate donor-stabilized tertiary silylium ions by protonation (Fig. 1A, iii) prompted us to target the synthesis of a secondary silylium ion by means of this strategy. Initially, we decided to use phenyl (Ph) as the leaving group because dephenylation (protodesilylation) proved to be a facile and fast process in our previous study (*27*). Treatment of a pale yellow suspension of benzenium ion $[C_6H_6{\cdot}H]^+[CHB_{11}H_5Br_6]^-$ in benzene with equimolar di-*tert*-butyl(phenyl) silane (**9**) at room temperature immediately resulted in a colorless solution from which an off-white solid precipitated. After 15 min, the solid was collected by filtration, washed with additional benzene, and dissolved in deuterated *ortho*-dichlorobenzene for nuclear magnetic resonance (NMR) spectroscopic analysis. Clean formation of the secondary silylium ion $tBu_2HSi^+[CHB_{11}H_5Br_6]^-$ (**8**) was observed (**9** → **8**; Fig. 2A, top left). The $^1H$ NMR spectrum showed a diagnostic signal at δ = 5.1 ppm with a $^1J$(Si,H) coupling constant of 233 Hz determined from the $^{29}Si$ satellites, revealing an intact Si–H bond. The associated doublet at δ = 73.0 ppm in the $^1H/^{29}Si$ heteronuclear single quantum coherence (HSQC) spectrum without decoupling in F1 dimension (fig. S6) was shifted downfield (Δδ = 59.8 ppm) relative to the hydrosilane substrate $tBu_2PhSiH$ (δ = 13.2 ppm), a clear indication for the development of silylium ion character. Unambiguous evidence for the structure of $tBu_2HSi^+[CHB_{11}H_5Br_6]^-$ (**8**) was eventually provided by crystallographic characterization (Fig. 2A, bottom). Single crystals suitable for x-ray diffraction were obtained from a solution of silylium carborane salt **8** in *ortho*-dichlorobenzene by vapor diffusion with

Institut für Chemie, Technische Universität Berlin, 10623 Berlin, Germany.
*Corresponding author. Email: hendrik.klare@tu-berlin.de (H.F.T.K.); martin.oestreich@tu-berlin.de (M.O.)

*n*-hexane at room temperature. The key geometric parameters are summarized in Table 1 and are discussed in comparison to the other obtained silylium ion species.

Careful NMR spectroscopic analysis of the protolysis of di-*tert*-butyl(phenyl)silane (**9**) revealed that traces of $t\mathrm{Bu_2PhSi^+}[\mathrm{CHB_{11}H_5Br_6}]^-$ also formed as a result of competitive Si–H bond cleavage. This tertiary dialkylarylsilylium ion exhibits higher solubility and can thus be separated from hydrogen-substituted silylium ion **8** by simple washing with small amounts of benzene. The chemoselectivity of dephenylation over dehydrogenation was determined to be higher than 95:5. The competing protolysis of the Si–H bond was not completely surprising, as we had already applied this process to the electrophilic C–H silylation of electron-rich (hetero)arenes (*30*). Hence, we considered the protolysis of a dihydrosilane as a complementary pathway for the generation of a secondary silylium ion. Indeed, dihydrogen gas immediately evolved from the reaction of di-*tert*-butylsilane (**7**) with equimolar amounts of the carborane acid, cleanly affording $t\mathrm{Bu_2HSi^+}[\mathrm{CHB_{11}H_5Br_6}]^-$ (**8**) as the sole product (**7** → **8**; Fig. 2A, top right).

To further probe the potential of our protolysis method, we next focused on the generation of a primary silylium ion. Both the dephenylation protocol (**10** → **12**; Fig. 2B, top left) and the dehydrogenation protocol (**11** → **12**; Fig. 2B, top right) proceeded smoothly, providing access to the primary counteranion-stabilized silylium ion $t\mathrm{BuH_2Si^+}[\mathrm{CHB_{11}H_5Br_6}]^-$ (**12**) from either *tert*-butyl(phenyl)silane (**10**) or *tert*-butylsilane (**11**). However, as a result of the volatility of the latter starting material [boiling point (b.p.) 34.4°C], the dephenylation process proved more practical. The measured $^1$H NMR chemical shift of δ = 5.0 ppm in deuterated *ortho*-dichlorobenzene was similar to that of $t\mathrm{Bu_2HSi^+}[\mathrm{CHB_{11}H_5Br_6}]^-$ (**9**), but a larger $^1J$(Si,H) coupling constant of 254 Hz was observed. The $^{29}$Si NMR resonance at δ = 27.0 ppm in the $^1$H/$^{29}$Si HSQC spectrum was shifted downfield relative to the starting material $t\mathrm{BuPhSiH_2}$ (δ = –14.5 ppm) and $t\mathrm{BuSiH_3}$ (δ = –39.7 ppm), but was shifted upfield (Δδ = 46 ppm) relative to secondary silylium ion **8**. Slow diffusion of *n*-hexane into a solution of $t\mathrm{BuH_2Si^+}[\mathrm{CHB_{11}H_5Br_6}]^-$ (**12**) in *ortho*-dichlorobenzene provided colorless crystals suitable for x-ray diffraction (Fig. 2B, bottom). The key parameters are discussed below.

Encouraged by the successful generation of both a secondary and a primary silylium ion, we then targeted the synthesis of the smallest member of hydrogen-substituted silylium ions, namely the elusive $\mathrm{H_3Si^+}$ cation. Although there are several theoretical and gas-phase studies on this heavier methylium congener (*24*–*26*), its synthesis in noncovalent form in the condensed phase has not yet been accomplished (*29*, *31*). In this case, both the hydride abstraction and the dehydrogenative protolysis approach (Fig. 2C,

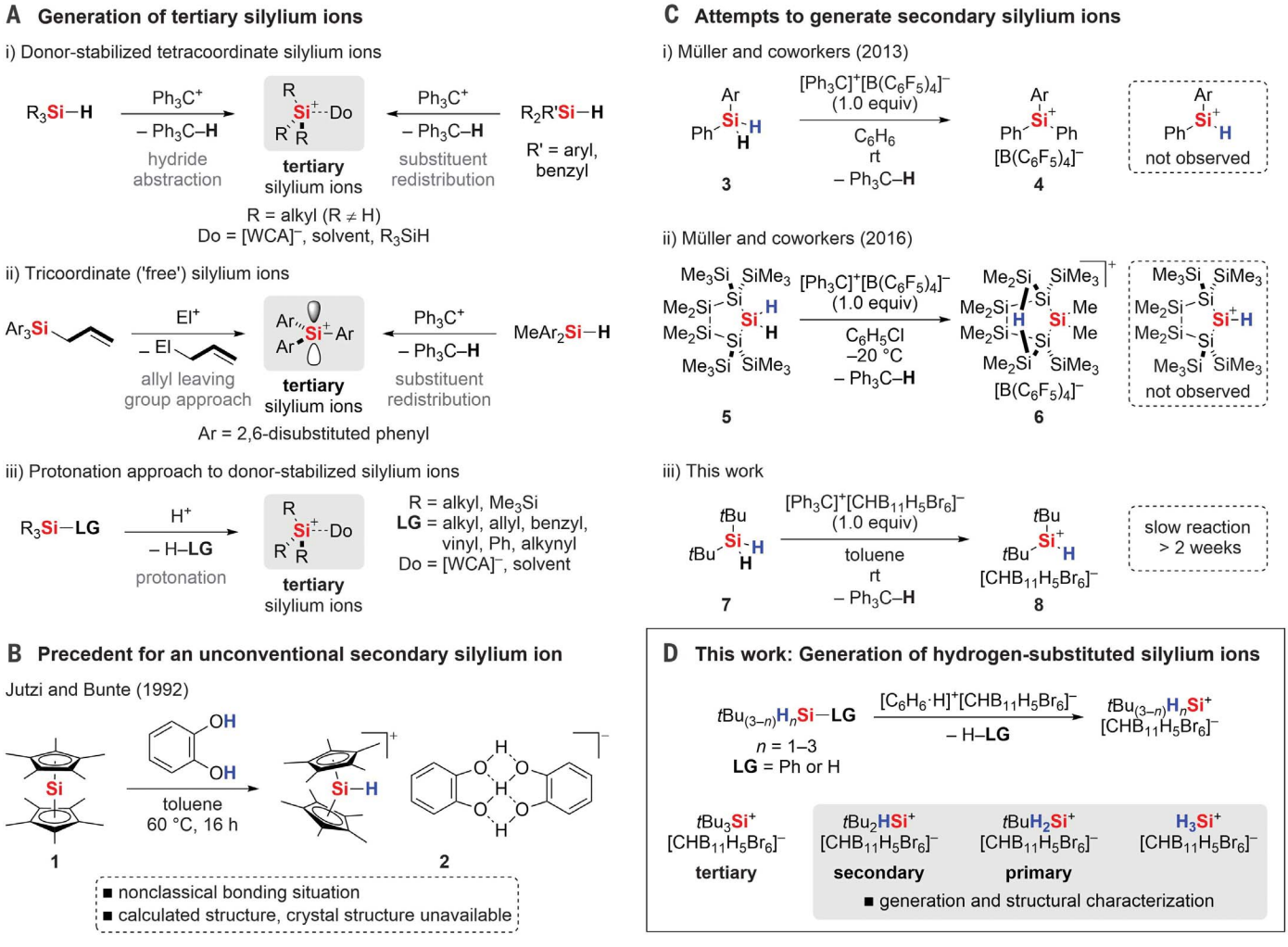


**Fig. 1. Synthetic routes to silylium ions.** (**A**) Reported methods to generate tertiary silylium ions ([WCA]$^-$ omitted for clarity) (*13*–*23*). (**B**) Jutzi and Bunte's synthesis of an unconventional secondary silylium ion (*7*, *8*). (**C**) Attempts to generate secondary silylium ions by hydride abstraction (*9*, *10*). (**D**) Our planned protolysis strategy to access hydrogen-substituted, counteranion-stabilized silylium ions. Do, donor; El, electrophile; LG, leaving group; Ph, phenyl; rt, room temperature; WCA, weakly coordinating anion.

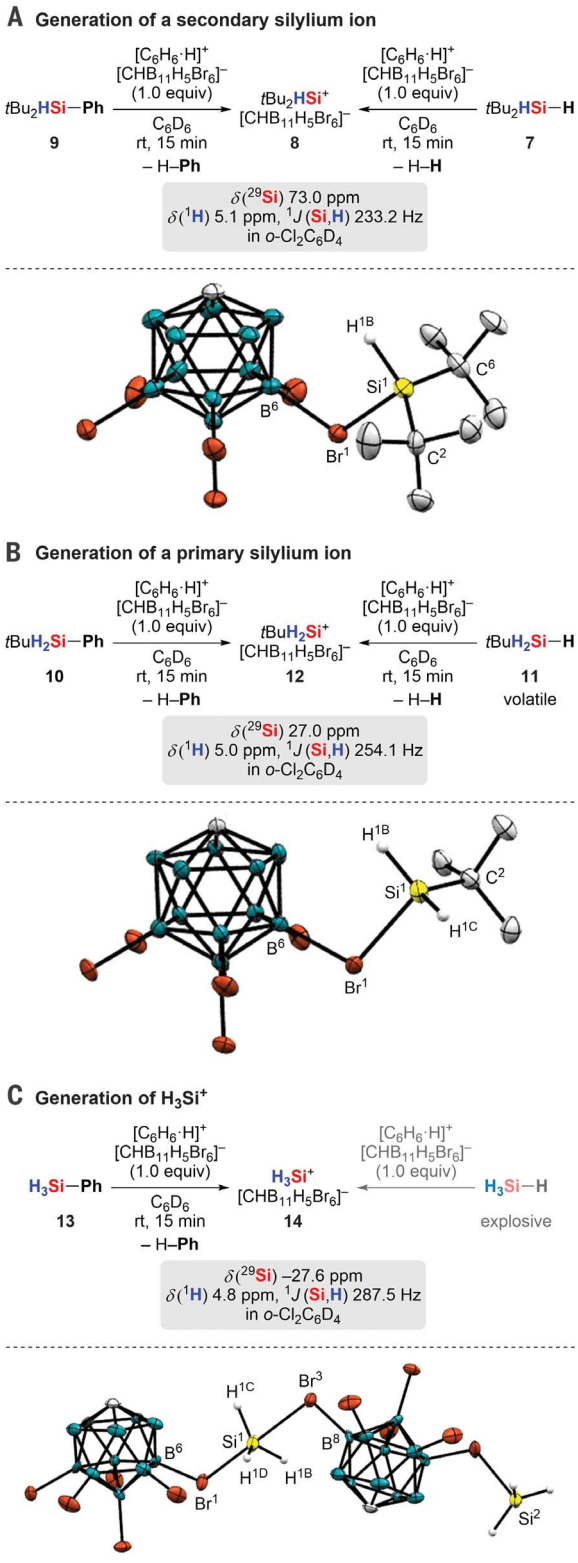


**Fig. 2. Synthesis and solid-state molecular structures of hydrogen-substituted, counteranion-stabilized silylium ions.** (**A**) Generation of a secondary silylium ion. (**B**) Generation of a primary silylium ion. (**C**) Generation of $H_3Si^+$.

top right) are impeded by the pyrophoric and explosive nature of monosilane ($SiH_4$) gas. Gratifyingly, the reaction of easy-to-handle phenylsilane (**13**; b.p. 120°C) with equimolar benzenium ion $[C_6H_6{\cdot}H]^+[CHB_{11}H_5Br_6]^-$ led again to selective Si–C($sp^2$) heterolysis and formation of $H_3Si^+[CHB_{11}H_5Br_6]^-$ (**14**) under release of benzene (Fig. 2C, top left). The poor solubility of this silylium ion in benzene facilitated its isolation, and **14** was obtained as an off-white solid in pure form after simple filtration and washing with small amounts of $C_6D_6$. The presence of three hydrogen substituents at the silicon atom was initially supported by the $^1H/^{29}Si$ HSQC spectrum in deuterated *ortho*-dichlorobenzene with coupling in F1 dimension, showing a quartet for the silicon atom at δ = –27.6 ppm with a $^1J$(Si,H) coupling constant of 287 Hz (fig. S27). The corresponding singlet at δ = 4.8 ppm in the $^1H$ NMR spectrum was again observed in a similar range as for the secondary and primary silylium ions **8** and **12**. The exclusively hydrogen-substituted silyl cation $H_3Si^+$ was found to have limited stability in solution, gradually transforming into $PhH_2Si^+$ by electrophilic C–H silylation of the benzene solvent and subsequent dihydrogen elimination (fig. S1). This reaction pathway had already been described by Müller and co-workers (see **3** → **4**, Fig. 1C) (*9*, *10*). Despite its high reactivity in aromatic solvents, we eventually succeeded in the crystallographic characterization of $H_3Si^+[CHB_{11}H_5Br_6]^-$ (**14**). Colorless crystals suitable for x-ray diffraction were grown from a benzene solution by vapor diffusion with *n*-hexane at room temperature (Fig. 2C, bottom). In the solid state, silylium carborane salt **14** is stable under inert atmosphere for several months at –30°C.

For higher sensitivity, $^{29}Si$ NMR chemical shifts were measured by $^1H/^{29}Si$ HSQC spectroscopy (Table 2). Using this technique with coupling in F1 dimension also allows for the determination of the number of hydrogen substituents at the silicon atom. The spectra were recorded in deuterated *ortho*-dichlorobenzene because the silylium carborane salts are not very soluble in benzene. The experimental $^{29}Si$ NMR chemical shifts were further supported by relativistic density functional theory (DFT) calculations. The agreement between measured and computed $^{29}Si$ NMR chemical shifts is excellent (fig. S35), confirming the high quality of the chosen computational protocol.

The $^{29}Si$ NMR chemical shifts of reported counteranion-stabilized tertiary trialkylsilylium ions of type $R_3Si^+[CHB_{11}H_5Br_6]^-$ (R = alkyl) are observed to be shifted downfield in the range of 93 to 113 ppm (Table 2 and table S2) (*14*–*16*, *23*). Whereas the experimental chemical shift of the tri-*tert*-butyl derivative is unavailable (*15*), the calculated value is 112.1 ppm (tables S1 and S2). Successive replacement of the *tert*-butyl substituents by hydrogen atoms leads to pronounced upfield shifts of 39 ppm (from $tBu_3Si^+$ to $tBu_2HSi^+$), 46 ppm (from $tBu_2HSi^+$ to $tBuH_2Si^+$), and 55 ppm (from $tBuH_2Si^+$ to $H_3Si^+$). Although the *tert*-butyl substituent might be expected to stabilize

**Table 1. Key geometric parameters for the molecular structures of silylium carboranes $tBu_{(3-n)}H_nSi^+[CHB_{11}H_5Br_6]^-$ ($n$ = 0 to 3).** For complete crystallographic data and details of structure refinement, see supplementary materials. Data for $tBu_3Si^+$ are from (*15*).

| | $tBu_3Si^+$ | $tBu_2HSi^+$ (8) | $tBuH_2Si^+$ (12) | $H_3Si^+$ (14) |
|---|---|---|---|---|
| Si–Br (Å) | 2.465 ± 0.005 | 2.4110 ± 0.0014 | 2.3777 ± 0.0016 | 2.477 ± 0.004 [$Br^1$]<br>2.770 ± 0.004 [$Br^3$] |
| B–$Br_{coord}$ (Å) | 2.04 ± 0.02 | 2.007 ± 0.005 | 2.017 ± 0.006 | 1.988 ± 0.015 [$Br^1$]<br>1.988 ± 0.016 [$Br^3$] |
| B–$Br_{uncoord}$ (Å) | 1.92–1.93 ± 0.02 | 1.937–1.958 ± 0.006 | 1.941–1.961 ± 0.006 | 1.923–1.959 ± 0.016 |
| Si–Br–B (°) | 125.0 ± 0.5 | 110.53 ± 0.16 | 104.42 ± 0.16 | 105.5 ± 0.4 [$Br^1$, $B^6$]<br>104.7 ± 0.4 [$Br^3$, $B^8$] |
| R–Si–R (°) | 117.7 ± 0.7 [$C^6$, $C^{10}$]<br>115.9 ± 0.6 [$C^2$, $C^6$]<br>115.1 ± 0.7 [$C^2$, $C^{10}$] | 121.7 ± 0.2 [$C^2$, $C^6$]<br>116 ± 2 [$C^2$, $H^{1B}$]<br>110 ± 2 [$C^6$, $H^{1B}$] | 117 ± 3 [$C^2$, $H^{1C}$]<br>114 ± 3 [$C^2$, $H^{1B}$]<br>111 ± 4 [$H^{1B}$, $H^{1C}$] | 119.1 ± 1.7 [$H^{1C}$, $H^{1D}$]<br>119.0 ± 1.7 [$H^{1B}$, $H^{1D}$]<br>118.8 ± 1.7 [$H^{1B}$, $H^{1C}$] |
| ∑R–Si–R (°) | 348.7 | 347.7 | 342 | 356.9 |
| Mean R–Si–R (°) | 116.2 | 115.9 | 114 | 119.0 |
| Br–Si–Br (°) | | | | 179.0 ± 0.2 |

**Table 2. Experimental and calculated $^{29}$Si NMR chemical shifts of silylium carboranes $R_3Si^+[CHB_{11}H_5Br_6]^-$.** Experimental values were determined by $^1$H/$^{29}$Si heteronuclear multiple quantum coherence (HMQC) NMR spectroscopy in 1,2-$Cl_2C_6D_4$ at 293 K. Fully relativistic 4c-mDKS/PBE0/IGLO-III/Dyall(TZ) calculations were performed at PBE0-D3(BJ)/def2-TZVPP/COSMO(1,2-$Cl_2C_6H_4$) structures.

| | $Me_3Si^+$ | $tBu_2HSi^+$ | $tBuH_2Si^+$ | $H_3Si^+$ |
|---|---|---|---|---|
| $\delta_{experimental}$($^{29}$Si) | 93.5 | 73.0 | 27.0 | –27.6 |
| $\delta_{calculated}$($^{29}$Si) | 85.9 | 74.5 | 24.5 | –21.5 |

the positive charge at the silicon atom by hyperconjugation, this effect is negligible because of the long C–Si bonds and less effective orbital overlap. Instead, more electronic charge is withdrawn from the silicon atom as a consequence of the higher electronegativity (χ) of the *tert*-butyl group relative to the hydrogen atom [χ(*t*Bu), 2.501; χ(H), 2.176] (*32*). Alkyl substitution thus leads to deshielding of the silicon nucleus in the $^{29}$Si NMR spectrum. This general trend is also consistent with calculations in the gas phase by Olsson and Cremer (*33*). However, a $^{29}$Si NMR chemical shift of δ = 270.2 ppm is expected for an ideal trigonal-planar, three-coordinate $H_3Si^+$ cation without any nucleophile interaction (*33*). The experimentally observed upfield shift is ascribed to counteranion as well as solvent coordination in the condensed phase and is in line with our and previous quantum chemical computations (*34*–*36*). For instance, even the approach of weak nucleophiles such as methane or benzene to the $H_3Si^+$ cation is predicted to lower the $^{29}$Si NMR chemical shift by 206 ppm (*36*) and 294 ppm (*33*), respectively.

We also analyzed $H_3Si^+[CHB_{11}H_5Br_6]^-$ by solid-state NMR spectroscopy using cross-polarization magic angle spinning (CPMAS) on the material identical to that characterized by x-ray crystallography (fig. S28). The recorded resonance at δ = –64.7 ppm corresponds to an upfield shift of Δδ = 37.1 ppm relative to the sample in *ortho*-dichlorobenzene, indicating breaking of the linear chain structure and solvation of the silylium carborane upon dissolution. A comparison of experimental and computed $^{29}$Si NMR chemical shifts (table S1) suggests that the counteranion-stabilized silylium ions exist as ion pairs in solution. However, we cannot fully exclude dynamic and, as such, partial exchange of the counteranion and the solvent because the chemical shifts slightly vary in *ortho*-dichlorobenzene and benzene. Deuterium incorporation into the carborane anion is in fact evidence of the formation of these deuterated arene adducts (*37*); these are at the same time strong Brønsted acids and a source of $D^+$, which in turn engages in electrophilic aromatic substitution of the carborane anion. H/D exchange at the silicon atom was not observed.

The $^1$H NMR chemical shifts of the hydrogen substituents at the silicon atom are observed in a narrow range of δ = 4.8 to 5.1 ppm, shifted downfield relative to the neutral tetracoordinate silane precursors. The increase of the $^1J$(Si,H) coupling constant from $tBu_2HSi^+$ (233 Hz) and $tBuH_2Si^+[CHB_{11}H_5Br_6]^-$ (254 Hz) to $H_3Si^+$ (287 Hz) is in agreement with the decreasing HOMO (highest occupied molecular orbital)–LUMO (lowest unoccupied molecular orbital) gap (table S3).

In accordance with the reported molecular structures of tertiary counteranion-stabilized trialkylsilylium ions $R_3Si^+[CHB_{11}H_5Br_6]^-$ [R = methyl (Me), ethyl (Et), isopropyl (*i*Pr), *t*Bu, $tBu_2Me$] (*14*–*16*, *23*), the positively charged silicon atom in secondary $tBu_2HSi^+[CHB_{11}H_5Br_6]^-$ (**8**) and primary $tBuH_2Si^+[CHB_{11}H_5Br_6]^-$ (**12**) is coordinated by one bromine atom from the pentagonal belt of the icosahedral carborane anion, leading to pyramidalization at the silicon atom (Fig. 2, A and B, bottom). The Si–Br bond lengths decrease from $tBu_3Si^+[CHB_{11}H_5Br_6]^-$ (2.465 Å) to **8** (2.411 Å) and **12** (2.377 Å). The reduced steric demand is likely to account for the stronger attractive interactions (*23*). However, the Si–Br bond distance of **12** is still elongated by more than 0.14 Å relative to the Si–Br bond in neutral bromosilane $Me_3SiBr$ (2.235 Å) (*38*), reflecting the weakly coordinating nature of the anion and the ionic character of silylium carborane salts **8** and **12**. Accordingly, the reduced steric bulk around the silicon atom and the formation of tighter contact ion pairs lead to more pronounced pyramidalization at the silicon atom, as indicated by the decreasing sum of all C–Si–C angles from $tBu_3Si^+[CHB_{11}H_5Br_6]^-$ (348.7°) to **8** (347.7°) and **12** (342°).

Intriguingly, the molecular structure of $H_3Si^+[CHB_{11}H_5Br_6]^-$ (**14**) differs markedly from these alkyl-substituted tetracoordinate silylium carborane salts (Fig. 2C, bottom). The $H_3Si^+$ cation is coordinated by two counteranions via the bromine atoms from the pentagonal belt of the carborane cluster, thereby forming linear polymeric chains with a Br–Si–Br angle of 179.0°. Hence, the pentacoordinate silicon atom is not pyramidalized but adopts a trigonal-planar (bipyramidal) geometry with an average of 119.0° and a sum of 356.9° for the H–Si–H bond angles. The two different Si–Br bond lengths of 2.477 Å and 2.770 Å reveal an unsymmetrical $H_3Si^+$ bonding. However, both distances are longer than those observed in the alkyl-substituted tetracoordinate silylium carboranes, reflecting the weak and noncovalent nature of these Si–Br interactions. Nonetheless, $H_3Si^+[CHB_{11}H_5Br_6]^-$ is preferably termed as a silanium ion, referring to a pentacoordinate silicon cation (*31*). The solid-state

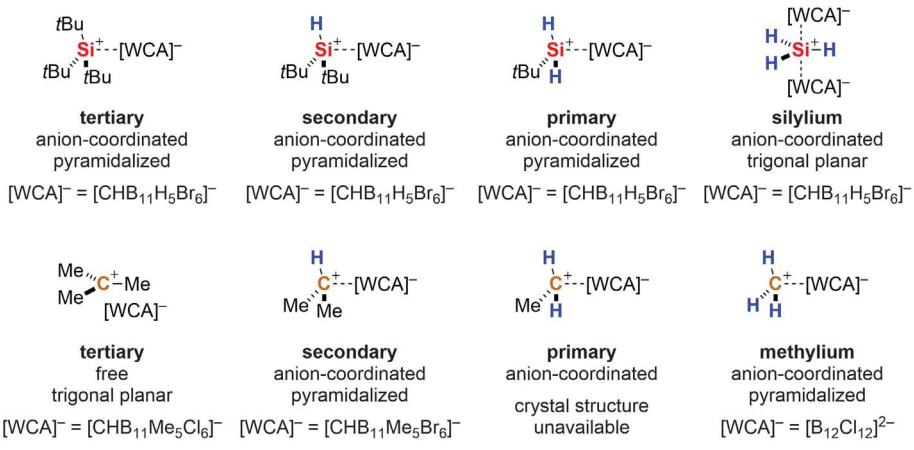


**Fig. 3. Comparison of carborane-stabilized silylium ions and reported carbenium ions.**

structure of $H_3Si^+[CHB_{11}H_5Br_6]^-$ is reminiscent of Reed's carborane acid $H^+[CHB_{11}H_5Br_6]^-$ (*39*), which suggests that $H_3Si^+$ can be viewed as a fat proton. That relation between silyl groups and protons had already been established by Fleming nearly 40 years ago (*40*).

A comparison of these silylium carboranes (*14–16*, *23*) with related carbenium salts (*41–43*) once again reveals the difference between silicon and carbon (*44*) despite their proximity in the periodic table (Fig. 3). Whereas the tertiary *tert*-butyl cation exists as a free carbenium ion as a result of hyperconjugation and polarization (*41*), these effects are impeded by the larger size and higher electrophilicity of the silicon atom, leading to stabilization by the counteranion and pyramidalization in the case of $R_3Si^+$ (R = Me, Et, *i*Pr, *t*Bu, $t$Bu$_2$Me) (*14–16*, *23*). The secondary and primary analogs are similar in both the carbenium and silylium ion series, featuring a tetracoordinate pyramidalized structure. However, the carbenium carboranes show more covalent bonding and halonium ion character that increases in the order *i*Pr < Et < Me (*42*). Notably, the smallest members of these reactive intermediates are distinctly different again: Whereas the methylium cation is covalent (*43*), the heavier $H_3Si^+$ analog is ionic and adopts a trigonal-planar (bipyramidal) geometry. Stabilization by two carborane counteranions through the typical coordination of the halide leads to a $H_3Si^+$-bridged linear chain structure. This bonding situation resembles exactly that of the corresponding Brønsted acid $H^+[CHB_{11}H_5Br_6]^-$ (*39*). Hence, the $H_3Si^+$ cation resembles a proton more than it resembles a methylium ion.

## REFERENCES AND NOTES


1. R. A. Moss, M. S. Platz, M. Jones Jr., Eds., *Reactive Intermediate Chemistry* (Wiley, 2004).
2. V. Ya. Lee, A. Sekiguchi, in *Organosilicon Compounds*, V. Ya. Lee, Ed. (Academic Press, 2017), vol. 1, pp. 197–230.
3. T. Müller, in *Functional Molecular Silicon Compounds I*, D. Scheschkewitz, Ed. (Springer, 2014), pp. 107–162.
4. G. A. Olah, *J. Org. Chem.* **66**, 5943–5957 (2001).
5. J. B. Lambert, Y. Zhao, *Angew. Chem. Int. Ed. Engl.* **36**, 400–401 (1997).
6. K.-C. Kim *et al.*, *Science* **297**, 825–827 (2002).
7. P. Jutzi, E.-A. Bunte, *Angew. Chem. Int. Ed. Engl.* **31**, 1605–1607 (1992).
8. T. Müller, P. Jutzi, T. Kühler, *Organometallics* **20**, 5619–5628 (2001).
9. C. Gerdes, W. Saak, D. Haase, T. Müller, *J. Am. Chem. Soc.* **135**, 10353–10361 (2013).
10. L. Albers, J. Baumgartner, C. Marschner, T. Müller, *Chem. Eur. J.* **22**, 7970–7977 (2016).
11. S. P. Fisher *et al.*, *Chem. Rev.* acs.chemrev.8b00551 (2019).
12. I. M. Riddlestone, A. Kraft, J. Schaefer, I. Krossing, *Angew. Chem. Int. Ed.* **57**, 13982–14024 (2018).
13. J. Y. Corey, *J. Am. Chem. Soc.* **97**, 3237–3238 (1975).
14. C. A. Reed, Z. Xie, R. Bau, A. Benesi, *Science* **262**, 402–404 (1993).
15. Z. Xie, R. Bau, A. Benesi, C. A. Reed, *Organometallics* **14**, 3933–3941 (1995).
16. Z. Xie *et al.*, *J. Am. Chem. Soc.* **118**, 2922–2928 (1996).
17. J. B. Lambert, S. Zhang, C. L. Stern, J. C. Huffman, *Science* **260**, 1917–1918 (1993).
18. J. B. Lambert, S. Zhang, S. M. Ciro, *Organometallics* **13**, 2430–2443 (1994).
19. S. P. Hoffmann, T. Kato, F. S. Tham, C. A. Reed, *Chem. Commun.* **2006**, 767–769 (2006).
20. J. B. Lambert, Y. Zhao, H. Wu, W. C. Tse, B. Kuhlmann, *J. Am. Chem. Soc.* **121**, 5001–5008 (1999).
21. A. Schäfer *et al.*, *Angew. Chem. Int. Ed.* **50**, 12636–12638 (2011).
22. A. Schäfer *et al.*, *Organometallics* **32**, 4713–4722 (2013).
23. L. Omann *et al.*, *Chem. Sci.* **9**, 5600–5607 (2018).
24. C. Maerker, P. R. Schleyer, in *The Chemistry of Organic Silicon Compounds, vol. 2*, Z. Rappoport, Y. Apeloig, Eds. (Wiley, 1998), pp. 513–555.
25. N. Goldberg, H. Schwarz, in *The Chemistry of Organic Silicon Compounds, vol. 2*, Z. Rappoport, Y. Apeloig, Eds. (Wiley, 1998), pp. 1105–1142.
26. S. Fornarini, in *The Chemistry of Organic Silicon Compounds, vol. 3*, Z. Rappoport, Y. Apeloig, Eds. (Wiley, 2001), pp. 1027–1057.
27. Q. Wu *et al.*, *Angew. Chem. Int. Ed.* **57**, 9176–9179 (2018).
28. O. Allemann, S. Duttwyler, P. Romanato, K. K. Baldridge, J. S. Siegel, *Science* **332**, 574–577 (2011).
29. A. R. Bassindale, T. Stout, *J. Organomet. Chem.* **271**, C1–C3 (1984).
30. Q.-A. Chen, H. F. T. Klare, M. Oestreich, *J. Am. Chem. Soc.* **138**, 7868–7871 (2016).
31. Y. Xiong, S. Yao, M. Driess, *Z. Naturforsch. B* **68**, 445–452 (2013).
32. N. Inamoto, S. Masuda, *Chem. Lett.* **11**, 1003–1006 (1982).
33. L. Olsson, D. Cremer, *Chem. Phys. Lett.* **215**, 433–443 (1993).
34. L. Olsson, C.-H. Ottosson, D. Cremer, *J. Am. Chem. Soc.* **117**, 7460–7479 (1995).
35. M. Arshadi, D. Johnels, U. Edlund, C.-H. Ottosson, D. Cremer, *J. Am. Chem. Soc.* **118**, 5120–5131 (1996).
36. C.-H. Ottosson, D. Cremer, *Organometallics* **15**, 5309–5320 (1996).
37. L. Omann *et al.*, *Angew. Chem. Int. Ed.* **57**, 8301–8305 (2018).
38. M. D. Harmony, M. R. Strand, *J. Mol. Spectrosc.* **81**, 308–315 (1980).
39. E. S. Stoyanov, S. P. Hoffmann, M. Juhasz, C. A. Reed, *J. Am. Chem. Soc.* **128**, 3160–3161 (2006).
40. I. Fleming, *Chem. Soc. Rev.* **10**, 83–111 (1981).
41. T. Kato, C. A. Reed, *Angew. Chem. Int. Ed.* **43**, 2908–2911 (2004).
42. T. Kato, E. Stoyanov, J. Geier, H. Grützmacher, C. A. Reed, *J. Am. Chem. Soc.* **126**, 12451–12457 (2004).
43. C. Bolli *et al.*, *Angew. Chem. Int. Ed.* **49**, 3536–3538 (2010).
44. S. Shaik, D. Danovich, W. Wu, P. C. Hiberty, *Nat. Chem.* **1**, 443–449 (2009).


## ACKNOWLEDGMENTS


We thank D. Stalke and A. N. Paesch for hosting the stay of Q.W. to obtain an improved set of crystallographic data for $H_3Si^+[CHB_{11}H_5Br_6]^-$ (Georg-August-Universität Göttingen); Q.-A. Chen for initial contributions to the dehydrogenation approach for silylium ion generation; L. Omann for sharing his expertise with Q.W.; and S. Kemper and J. D. Epping for expert advice with the NMR spectroscopic measurements (all Technische Universität Berlin). **Funding:** Supported by an Alexander von Humboldt Foundation postdoctoral fellowship (2017–2019) (Q.W.) and by an Einstein Foundation Berlin endowed professorship (M.O.). The computational work was supported by the Deutsche Forschungsgemeinschaft (SFB 1109, project A3). **Author contributions:** All experiments were conducted by Q.W. X-ray diffraction analysis was performed by E.I. Computations were run by R.M. and led by M.K. H.F.T.K. and M.O. directed the project and co-wrote the manuscript. **Competing interests:** The authors declare no competing financial interests. **Data and materials availability:** X-ray crystallographic data are available free of charge from the Cambridge Crystallographic Data Centre: CCDC 1913125 for $t$Bu$_2$HSi$^+[CHB_{11}H_5Br_6]^-$ (**8**), CCDC 1913126 for $t$BuH$_2$Si$^+[CHB_{11}H_5Br_6]^-$ (**12**), and CCDC 1913127 for $H_3Si^+[CHB_{11}H_5Br_6]^-$ (**14**), respectively. All other data are available in the main text or the supplementary materials.


## SUPPLEMENTARY MATERIALS

science.sciencemag.org/content/365/6449/168/suppl/DC1
Materials and Methods
Figs. S1 to S35
Tables S1 to S5
References (*45–73*)

4 May 2019; accepted 17 June 2019
10.1126/science.aax9184

# Characterization of hydrogen-substituted silylium ions in the condensed phase

Qian Wu, Elisabeth Irran, Robert Müller, Martin Kaupp, Hendrik F. T. Klare and Martin Oestreich

*Science* **365** (6449), 168-172.
DOI: 10.1126/science.aax9184

**An acidic route to silicon cations**

The simplest silicon cation, with a central Si atom bonded to just three hydrogens, has long eluded bulk synthesis. Wu *et al.* now report a straightforward route to this molecule by reacting a carborane acid with phenyl silane, producing benzene and the silylium carborane ion pair. A similar protocol offered efficient syntheses of primary and secondary silyl cations through acidic cleavage of Si–phenyl or Si–H bonds. All three products, characterized crystallographically and in solution, manifested weak coordination to bromine substituents of the carboranes.

*Science*, this issue p. 168